# Ponderomotive Effects on Angular Distributions of Photoelectrons

R. R. Freeman, T. J. McIlrath,[a] P. H. Bucksbaum, and M. Bashkansky[b]
*AT&T Bell Laboratories, Murray Hill, New Jersey 07974*
(Received 2 September 1986)

We report the observation of intensity-dependent angular distributions of photoelectrons in multiphoton ionization of xenon by 1064-nm light in the intensity range of $(0.5-5)\times10^{13}$ W/cm$^2$. The intensity dependence is shown to arise from the scattering of the photoelectrons from the ponderomotive potential created by the intense optical fields. This phenomenon is a general, final-state effect which can severely restrict the usefulness of angular distribution measurements in high-intensity multiphoton ionization.

PACS numbers: 32.80.Rm, 41.70.+t

The angular distribution of photoelectrons in linear spectroscopy is an important tool in the study of bound- and continuum-state wave functions. In nonresonant multiphoton ionization (MPI) there are no intermediate-state resonances and extremely high laser intensities are required to observe ionization. A number of new phenomena accompany the ionization process at these intensities, the most dramatic of which is above-threshold ionization (ATI),[1] where photoelectrons are produced at several discrete kinetic energies separated by the photon energy $h\nu$. Figure 1 is a schematic of the ATI process for xenon irradiated by intense 1064-nm light.

Although ATI has been studied by numerous investigators, little attention has been given to another, more subtle effect of the use of high-intensity light in MPI experiments: the repulsion of photoelectrons from the focus of the laser by the ponderomotive potential. In this paper we show that this effect dominates the angular distribution of photoelectrons in high-intensity MPI experiments and, as a consequence, largely masks any results that depend upon the physics of the atom or of the transition process.

The apparatus has been described elsewhere[2]; briefly, a 100-psec, transform-limited pulse of 1064-nm light at 10 Hz was focused to nearly the diffraction limit inside a vacuum vessel. The intensity distribution at the focus was measured with a charge-coupled-device array and continuously monitored with a television camera. The average pulse energy was held constant to within $\pm 2\%$. The interaction region and the time-of-flight electron-energy analyzer were shielded from stray electric and magnetic fields. The angular resolution of the photoelectron detector was 3°, and the energy resolution was 10 meV at 1 eV. Space-charge effects remained completely negligible for all the data reported here.

The energy spectrum of ATI electrons recorded for xenon at 1064 nm at a peak intensity of $2\times10^{13}$ W/cm$^2$ is shown in Fig. 2. Data were recorded for intensities between $5\times10^{12}$ and $5\times10^{13}$ W/cm$^2$. Above a threshold value of about $1\times10^{13}$ W/cm$^2$, the overall shape of this spectrum was relatively insensitive to the intensity of the laser. Although the individual ATI peaks broadened with increasing intensity, there was no overall shift in energy position. Contrary to a recent report,[3] no ATI peak decreased in absolute magnitude as the laser power was increased.

Figure 3(a) shows the intensity dependence of the angular distribution of ATI electrons. The data were taken

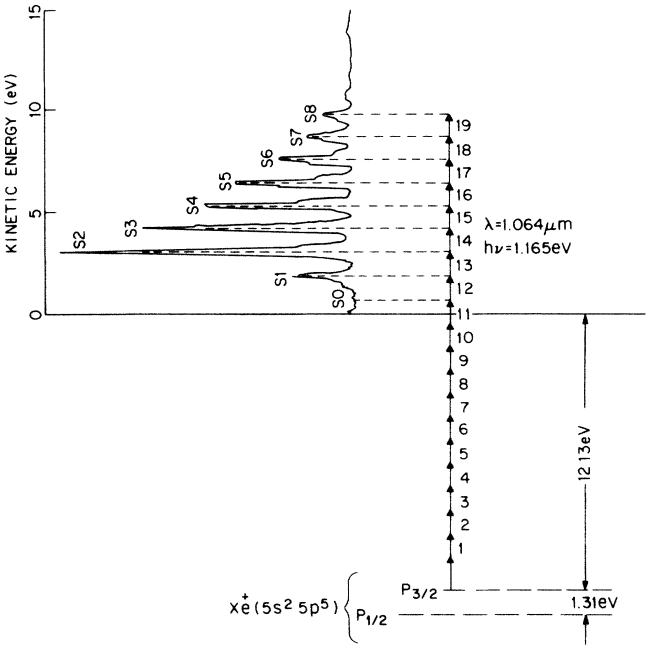


FIG. 1. A schematic of the ATI process for xenon irradiated by intense 1064-nm light. The (doublet) peaks are labeled by S$N$ where $N$ is the number of photons absorbed beyond that just necessary to ionize the atom at low intensities. The energy scale is the kinetic energy of the free electron. The two negative-energy initial states represent the two ion-core states which are placed below zero by their ionization energy. They are thus inverted from the normal Xe II diagrams. Only the absorption from the $P_{3/2}$ core is shown since absorption data at 532 nm indicate that this channel is dominant, although at 1064 nm the widths of the peaks preclude identification of the separate channels. The angular distribution model used here does not depend upon the ion-core state.

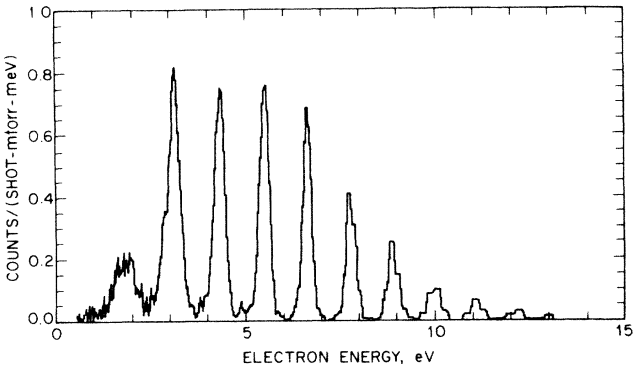


FIG. 2. A typical ATI energy system recorded for xenon irradiated at 1064 nm at a peak intensity of approximately $2\times10^{13}$ W/cm$^2$. The first observable peak at about 1.8 eV is S1. The S0 peak was not observed for 1064-nm radiation but was prominent in ATI spectra recorded with use of 532-nm data. These data were taken with the detector aligned with the electric field of the light. The ordinate is normalized to counts/(shot·mTorr·meV).

for a nearly Gaussian beam, and all measurements were made in the plane normal to the direction of light propagation. The angle in Fig. 3 is measured between the polarization of the light and the direction of the detector. At low intensities the angular distribution for all the ATI peaks is highly peaked along the polarization vector; as the intensity is increased, the angular distribution of photoelectrons tends to become isotropic. This effect is strongest for the lowest energy peaks, becoming progressively less for the higher-order peaks. We believe that this phenomenon of *intensity-dependent* angular distributions is due to photoelectron scattering from the ponderomotive potential created by the intense field of the ionizing laser. This conclusion is reinforced by the observation that the angular distribution depends on the shape of the focus as well as on the light intensity.

The response of free electrons to an intense electromagnetic wave has been discussed in detail by many authors[4] and is well understood. Electrons of charge $q$ and mass $m$, driven sinusoidally at the frequency $\omega$ of the optical wave with peak field $E_0$, scatter elastically from regions of high intensity as though there were a potential, known as the *ponderomotive* potential, whose magnitude is just the quiver kinetic energy

$$q^2E_0^2/4m\omega^2. \quad (1)$$

Attempts to scatter electrons from standing-wave laser beams in the 1960's were probably the first to observe directly ponderomotive scattering.[5]

Several authors have shown that the high Rydberg states and the ionization threshold of an atom in a low-frequency optical field have a Stark shift upward in an optical field given by (1), while the atom's ground state has a much smaller shift.[6] The ionization potential of an atom is thus *increased* by the local ponderomotive ener-

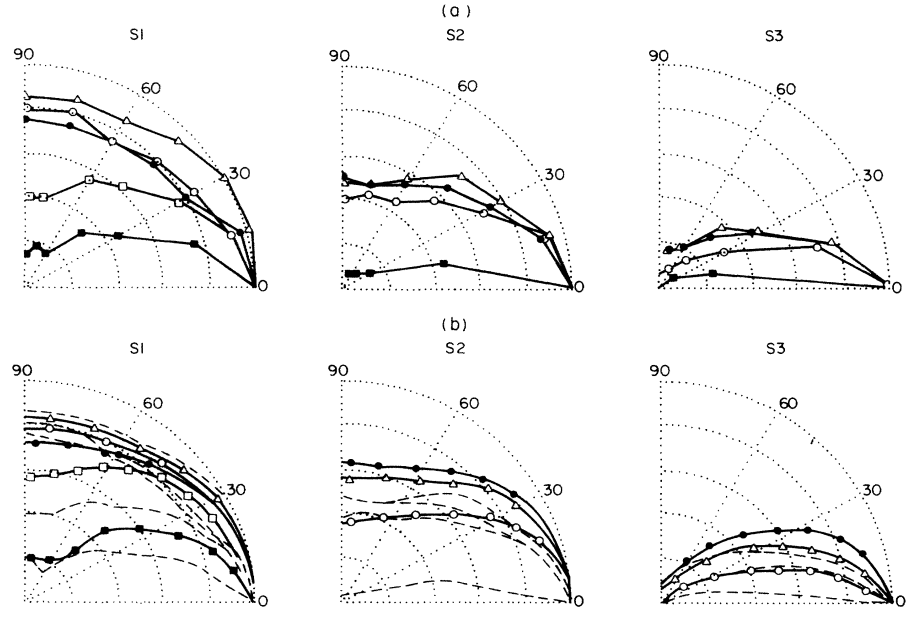


FIG. 3. (a) Angular distribution data for peaks S1, S2, and S3 as a function of intensity; the intensity values for the symbols are (1.5, 2.25, 3, 4.5, and 6)$\times10^{13}$ W/cm$^2$ for the closed square, open square, closed circle, open circle, and triangle, respectively. (b) The results of the model calculations invoking ponderomotive scattering. The calculations are the solid lines with the corresponding symbols from (a), and the data from (a) are indicated by means of dashed lines. The model calculations were not performed for the lowest intensities for S2 and S3. For these data the ponderomotive force is cylindrically symmetric and affects the slower electrons more than the faster ones.

gy. The ponderomotive energy converts into kinetic energy as the electron leaves the light beam, just compensating for the decrease in the initial kinetic energy due to the raised ionization potential.[7] Because all measurements are made *outside* of the beam, the recorded energy of electrons in a given ATI electron peak (i.e., all electrons which have absorbed a given number of photons in the ionization process) will, in first order, be independent of the light intensity. Boreham and his colleagues[8] have used ponderomotive forces to model the energy distribution of electrons ($>50$ eV) produced in the multiphoton ionization of atoms by high-intensity beams under collision-free conditions. However, because of the conservative nature of the ponderomotive potential for cw or long-pulse laser beams, the search for unambiguous evidence of electron-light scattering in the energy spectrum of multiphoton-ejected electrons has been difficult and largely unrewarding. But whereas free electrons do not absorb energy on scattering from a static ponderomotive potential, they do absorb momentum readily. Thus changes in the trajectory of free electrons are a much more sensitive monitor of ponderomotive forces.

The angular distributions of the ATI peaks depend experimentally upon the intensity of the laser light, the kinetic energy of the ionized electrons, and the spatial distribution of the laser intensity. These results can be quantitatively reproduced with a simple model of ionization followed by electron propagation in the ponderomotive potential. The model is based upon the following physical assumptions: 1. The initial angular distribution of the electrons is assumed to be intensity independent and equal to the values we measured at low intensities: about 12° opening angle about the polarization direction for the lowest ATI peaks down to 4° for the higher peaks. 2. As a result of the highly nonlinear nature of the ionization, the atoms tend to ionize within a narrow range of intensities,[9] so that the electrons of a given ATI peak are assumed to be produced uniformly along equal-intensity surfaces of the focused beam. 3. The *initial* kinetic energy of the electrons is assumed to be $E_{\text{init}} = E_{\text{final}} - E_{\text{pond}}$, where $E_{\text{final}}$ is the detected energy and $E_{\text{pond}}$ is the value of the ponderomotive potential at the intensity at which the electrons are created via ionization. 4. The radial light distribution at a distance $z$ from the focus is taken to be

$$I(r,z,t) = \frac{I_0}{r(z)^2} e^{-[r/r(z)]^2} e^{-[(t-z/c)/\tau]^2}, \tag{2}$$

where $r(z)^2 = w^2[1+(\lambda z/\pi w^2)^2]$, $\tau$ is the pulse length, and $w$ is the spot size at the focus. The values for $w$, $I_0$, and $\tau$ were determined by direct measurement; an intensity of $1\times10^{13}$ W/cm$^2$ yields a ponderomotive potential of 1.04 eV for 1064-nm radiation. The radial force resulting from (2) is proportional to

$$F(r,z,t) \sim [2r/r(z)^2] I(r,z,t). \tag{3}$$

Note that this force does not depend upon the polarization or the direction of propagation of the laser beam, but does depend upon time.

The trajectories of a large number of electrons throughout the confocal volume were computed by means of Eq. (3), and the angular distribution for each ATI peak was calculated by averaging over the final angles of all the electrons. The only unknown in this simulation was the value of the intensity at which the electrons in each ATI peak were created: This one number was adjusted for each ATI peak for the best fit to the data at one intensity. The angular distributions for each ATI peak at all other intensities were calculated without further adjustment of any parameters. The results, which are in substantial agreement with the data, are shown on Fig. 3(b).

The ATI peaks S1, S2, and S3 have final energies of 1.6, 2.7, and 3.8 eV, respectively; the corresponding values for $E_{\text{pond}}$ obtained from fitting to the data are 1.5, 2.6, and 2.8 eV. These numbers suggest a consistent and satisfying picture of the high-order ionization process in the time-varying envelope of the laser pulse. None of the neutral atoms experience an intensity above the saturation value, approximately $2.8\times10^{13}$ W/cm$^2$ (2.8 eV) as determined from our data. The saturation intensity is also the intensity at which most of the electrons are made, and this determines the value of $E_{\text{pond}}$ for S3 and above. However, electrons cannot be made at an intensity corresponding to a ponderomotive energy greater than the corresponding $E_{\text{final}}$. Thus S1 and S2 electrons will be created (at a substantially reduced rate) at the highest intensity at which these channels are still open, namely at a value of $E_{\text{pond}}$ which is slightly less than $E_{\text{final}}$.

The ability of the model to predict the angular distributions of the ATI peaks when the spatial distribution of the laser beam was significantly distorted was also checked. An elliptical spot was produced at the focus with a ratio of major to minor axes of about 3:1. Here the ponderomotive force was strongest along the minor axes of the ellipse. All the relevant beam parameters were directly measured, and the angular distributions for the case of the light polarization along the major axis of the ellipse were recorded. Figure 4 shows the results of the measurements; also shown are the predictions of the model, computed without any adjustable parameters (i.e, with use of the same values for $E_{\text{pond}}$ obtained in the circular-beam-spot measurement). The model simulations satisfactorily reproduce the distorted angular distributions. In further experiments with the elliptical beam, we found that if the polarization direction is kept fixed, then a rotation of the axes of the ellipse rotates the angular distribution of the photoelectrons.

We conclude that photoelectron angular distributions at high intensity depend explicitly upon the macroscopic intensity distribution of the light and not just the local intensity at the atoms. We have shown that as a result

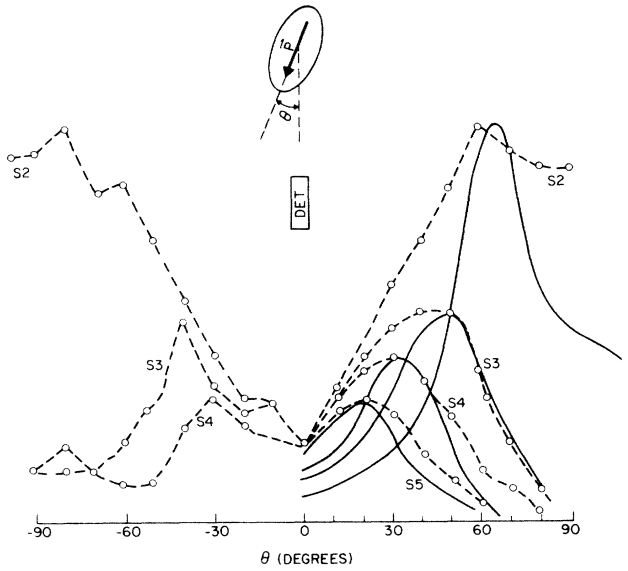


FIG. 4. The experimental distribution of photoelectrons as a function of angle from the direction of the axis for an elliptical beam with a 3:1 eccentricity with the axis of the ellipse parallel to the electric field polarization. Here the ponderomotive force is no longer cylindrically symmetric, being strongest along the minor axis of the ellipse. Also shown are the results of the model calculation that uses parameters determined from the circular-focus fits. The calculation has been normalized in height for each S/N peak.

of ponderomotive forces which are inherent in the technique, the angular distribution of photoelectrons produced by MPI caused by long-wavelength, high-intensity lasers is primarily determined by the spatial distribution of the laser beam near the focus. Under these conditions, extreme care must be taken to try to relate angular distributions of photoelectrons to the target species' wave functions or to the properties of the transition moments.

One of us (T.J.M.) acknowledges the partial support of the National Science Foundation under Grant No. CPE 81-19250.

[a]Permanent address: Institute of Physical Science and Technology, University of Maryland, College Park, MD 20742.

[b]Present address: Physics Department, Columbia University, New York, NY 10027.

[1]P. Agostini, F. Fabre, G. Mainfray, G. Petite, and N. K. Rahman, Phys. Rev. Lett. **42**, 1127 (1979); P. Kruit, J. Kimman, and M. J. van der Wiel, J. Phys. B **14**, L597 (1981).

[2]P. H. Bucksbaum, M. Bashkansky, R. R. Freeman, T. J. McIlrath, and L. F. DiMauro, Phys. Rev. Lett. **56**, 2590 (1986).

[3]L. A. Lompré, A. L'Huillier, G. Mainfray, and C. Manus, J. Opt. Soc. Am. B **12**, 1906 (1985).

[4]T. W. Kibble, Phys. Rev. **150**, 1060 (1966); J. H. Eberly, Prog. Opt. **7**, 359 (1969); H. Hora, *Physics of Laser Driven Plasmas* (Wiley, New York, 1981); M. Mittleman, *Introduction to the Theory of Laser-Atom Interactions* (Plenum, New York, 1982).

[5]L. S. Bartell, H. B. Thompson, and R. R. Roskos, Phys. Rev. Lett. **14**, 851 (1965).

[6]P. Avon, C. Cohen-Tannoudji, J. Dupont-Roc, and C. Fabre, J. Phys. (Paris) **37**, 993 (1976); M. H. Mittleman, Phys. Rev. A **29**, 2245 (1984).

[7]H. G. Muller, A. Tip, and M. J. van der Wiel, J. Phys. B **16**, L679 (1983).

[8]B. W. Boreham and H. Hora, Phys. Rev. Lett. **42**, 776 (1979); B. W. Boreham and J. L. Hughes, Zh. Eksp. Teor. Fiz. **80**, 496 (1981) [Sov. Phys. JETP **53**, 252 (1981)].

[9]P. Lambropoulos, Phys. Rev. Lett. **55**, 2141 (1985).